

Long non-coding RNA *MEG3* inhibits adipogenesis and promotes osteogenesis of human adipose-derived mesenchymal stem cells via miR-140-5p

Zheng Li¹ · Chanyuan Jin¹ · Si Chen¹ · Yunfei Zheng² · Yiping Huang² · Lingfei Jia^{3,4} · Wenshu Ge^{5,6} · Yongsheng Zhou^{1,6}

Received: 6 February 2017 / Accepted: 15 March 2017 / Published online: 5 April 2017
© Springer Science+Business Media New York 2017

Abstract lncRNAs are an emerging class of regulators involved in multiple biological processes. *MEG3*, an lncRNA, acts as a tumor suppressor, has been reported to be linked with osteogenic differentiation of MSCs. However, limited knowledge is available concerning the roles of *MEG3* in the multilineage differentiation of hASCs. The current study demonstrated that *MEG3* was downregulated during adipogenesis and upregulated during osteogenesis of hASCs. Further functional analysis showed that knockdown of *MEG3* promoted adipogenic differentiation, whereas inhibited osteogenic differentiation of hASCs. Mechanically, *MEG3* may execute its role via regulating miR-140-5p. Moreover, miR-140-5p was upregulated during adipogenesis and downregulated during osteogenesis in hASCs, which was negatively correlated with *MEG3*. In conclusion, *MEG3* participated in the balance

of adipogenic and osteogenic differentiation of hASCs, and the mechanism may be through regulating miR-140-5p.

Keywords lncRNA · miRNA · *MEG3* · miR-140-5p · Human adipose-derived stem cells · Adipogenesis · Osteogenesis

Abbreviations

lncRNA	Long non-coding RNA
MSCs	Mesenchymal stem cells
hASCs	Human adipose-derived stem cells
<i>MEG3</i>	Maternally expressed gene 3
ncRNA	Non-coding RNA
miRNA	microRNA
<i>BMP2</i>	Bone morphogenetic protein 2
<i>BMP4</i>	Bone morphogenetic protein 4
ALP	Alkaline phosphatase
ARS	Alizarin red staining
<i>OCN</i>	Osteocalcin
<i>RUNX2</i>	Runt-related transcription factor 2
<i>CEBP1α</i>	CCAAT-enhancer-binding proteins-α
<i>TGFβ</i>	Transforming growth factor β

Zheng Li and Chanyuan Jin have contributed equally to this article.

Electronic supplementary material The online version of this article (doi:10.1007/s11010-017-3015-z) contains supplementary material, which is available to authorized users.

✉ Lingfei Jia
jialingfei1984@sina.com

✉ Wenshu Ge
esther1234@bjmu.edu.cn

¹ Department of Prosthodontics, Peking University School and Hospital of Stomatology, Beijing 100081, China

² Department of Orthodontics, Peking University School and Hospital of Stomatology, Beijing 100081, China

³ Department of Oral and Maxillofacial Surgery, Peking University School and Hospital of Stomatology, Beijing 100081, China

⁴ Central Laboratory, Peking University School and Hospital of Stomatology, 22 Zhongguancun Avenue South, Haidian District, Beijing 100081, China

⁵ Department of General Dentistry 2, Peking University School and Hospital of Stomatology, 22 Zhongguancun South Avenue, Haidian District, Beijing 100081, China

⁶ Beijing Key Laboratory of Digital Stomatology, National Engineering Lab for Digital and Material Technology of Stomatology, Beijing 100081, China

PPAR γ Peroxisome proliferator-activated receptor- γ
GAPDH Glyceraldehyde 3-phosphate dehydrogenase

Introduction

As a promising cell type for bone or adipose tissue engineering, hASCs have the capacity of differentiating into several lineages including osteoblasts and adipocytes [1]. It has been demonstrated that a mutually exclusive relationship exists between adipogenesis and osteogenesis in hASCs [2]. Thus, to facilitate feasible and effective applications in tissue engineering, further investigations of the molecular mechanisms in the adipocyte and osteoblast differentiation of hASCs are needed [3].

Non-coding RNAs (ncRNAs), which own no protein-coding capabilities, have been reported to participate in a myriad of biological and pathological processes. As main types of small ncRNAs, microRNAs (miRNAs) are 22 nucleotides in length, regulating gene expressions by directly binding to the 3'-UTR region of mRNAs directly [4, 5]. Another critical members, lncRNAs, are greater than 200 nt in length, exhibiting poor sequence conservation and function through various mechanisms [6]. Recent studies have demonstrated that lncRNAs may modulate target genes through regulating miRNAs in post-transcriptional level. For example, human periodontal mesenchymal stem cells (hPDLSCs) osteogenesis impairment-related lncRNA (lncRNA-POIR) positively modulated the osteogenic differentiation of hPDLSCs through regulating miR-182 [7]. Increasing researches showed that several miRNAs were involved in the balance of adipogenesis and osteogenesis, including miR-204 [8], miR-637 [9], and miR-194 [10]. Moreover, lncRNAs, such as *HOTAIR* [11], *ADNCR* [12], and *H19* [3], have been identified to play critical parts in the adipogenic and osteogenic differentiation of MSCs.

As one of lncRNAs, *MEG3* is widely expressed in many normal tissues and often represents as a tumor suppressor in several carcinomas, including hepatocellular carcinoma and glioma [13–15]. Researches have also showed its potential role in the angiogenesis [16] and vascular function pathological processes of diabetes [17]. Lately, it has been demonstrated that *MEG3* was involved in osteogenesis of MSCs partly by activating *BMP4* transcription [18]. However, the functions and roles of *MEG3* in the adipocyte and osteoblast differentiation of hASCs are not well understood and the specific mechanisms still remain largely elusive.

In this study, we demonstrated that *MEG3* inhibited adipogenic differentiation of hASCs, whereas promoted osteogenic differentiation. Moreover, consistent with the previous study that miR-140-5p suppressed BMP2-mediated osteogenesis in undifferentiated hMSCs [19], we found that miR-140-5p enhanced adipogenic

differentiation and decreased osteogenic differentiation of hASCs, which was negatively correlated with *MEG3*. Then we tested the relationship between *MEG3* and miR-140-5p, and proposed that *MEG3* may regulate adipocyte and osteocyte differentiation of hASCs at least partly via miR-140-5p. This study provided better understanding of the molecular basis of adipogenic and osteogenic differentiation of hASCs and offered new potential target sites for adipose and bone tissue engineering.

Materials and methods

Cell culture

Primary hASCs were obtained from ScienCell Research Laboratory (Carlsbad, CA, USA) from three different donors. Cells between three and five passages were used for the experiments and all in vitro experiments were repeated in triplicate. hASCs were cultured in proliferation medium (PM) made up of DMEM supplemented with 10% fetal bovine serum and 1% antibiotics at 37 °C in an incubator, with an atmosphere of 95% air, 5% CO₂, and 100% relative humidity. For the adipogenic differentiation, cells were allowed to be confluent for 1 day, and then cultured in standard proliferation medium supplemented with 50 nM insulin, 100 nM dexamethasone, 0.5 mM 3-isobutyl-1-methylxanthine, and 200 μ M indomethacin. For the osteogenic differentiation, cells were induced using standard proliferation medium supplemented with 100 nM dexamethasone, 200 mM L-ascorbic acid, and 10 mM β -glycerophosphate. All materials were obtained from Sigma-Aldrich (St. Louis, MO, USA) unless otherwise stated.

Lentiviral transfection

Recombinant lentiviruses targeting *MEG3* (sh-*MEG3*), negative control (NC), miR-140-5p mimics, miRNA negative control (miR-NC), miR-140-5p inhibitor (Anti-miR-140-5p), and miR-140-5p inhibitor negative control (Anti-NC) were obtained from Integrated Biotech Solutions Co. (Ibsbio Co., Shanghai, China). Lentiviral infection was performed as described previously [20]. Transfection was conducted by exposing hASCs to the viral supernatant at a multiplicity of infection of 100 for 24 h, followed by selection with Puromycin (Sigma-Aldrich) at 1 μ g/ml. The sequences used for *MEG3* knockdown, miR-140-5p overexpression, and knockdown are shown in Table 1.

Table 1 Sequences of RNA and DNA Oligonucleotides

Name	Sense strand/sense primer (5'–3')	Antisense strand/antisense primer (5'–3')
Primers for qRT-PCR		
<i>MEG3</i>	GAGTGTTCCCTCCCAAGG	GCGTGCCTTTGGTGATTGAG
miR-140-5p primer	AUGGUAUCCCAUUUUGGUGAC	AAAAATATGGAACGCTTCACGAATG
<i>RUNX2</i>	CCGCCTCAGTGATTTAGGGC	GGGTCTGTAATCTGACTCTGTCC
<i>OCN</i>	CACTCCTCGCCCTATTGGC	CCCTCCTGCTTGACACAAAAG
<i>GAPDH</i>	GGTACCAGGGCTGCTTTT	GGATCTCGCTCCTGGAAGATG
<i>U6</i>	GGGCAGGAAGAGGGCCTAT	AAAAATATGGAACGCTTCACGAATG
<i>PPARγ</i>	GCTGTTATGGGTGAAACTCTG	ATAAGGTGGAGATGCAGGTTC
<i>CEBPα</i>	GCAAGGCCAAGAAGTCGGTGGC	TGCCCATGGCCTTGACCAAGGG
shRNA		
sh- <i>MEG3</i>	CCCUCUUGCUUGUCUUACUTT	
NC	TTCTCCGAACGTGTCACGTTTC	
miR-140-5p mimics	CAGTGGTTTTACCCTATGGTAG	
miR-NC	UUCUCCGAACGUGUCACGUTT	
Anti-miR-140-5p	CTACCATAGGGTAAAACCACTG	
Anti-NC	CAGUACUUUUGUGUAGUACAA	

Oil Red O staining and quantification

After 10 days of adipogenic differentiation, cells were washed with phosphate-buffered saline (PBS) and fixed in 10% formalin for 30 min. The cells were then rinsed with 60% isopropanol. Oil Red O (0.3%, Sigma-Aldrich) was added and incubated for 10 min with gentle agitation. After staining, the cells were washed with distilled water to remove unbound dye, visualized by light microscopy, and photographed. For quantitative assessment, the Oil Red O was eluted by 100% isopropanol and quantified by spectrophotometric absorbance at 520 nm accompanied with blank solution (100% isopropanol).

Alkaline phosphatase (ALP) staining and activity

ALP staining and activity were performed as described previously [21]. After 7 days of osteogenic induction, cells were washed three times with phosphate-buffered saline (PBS) and then fixed with 4% paraformaldehyde at room temperature for 10 min. Then, the samples were kept in dark place to undergo ALP staining for 20 min (CW BIO, Beijing, China), followed by three times washing with PBS. Images were obtained with a scanner. ALP activity was analyzed using an ALP Assay Kit (Nanjing Jiancheng Bioengineering Institute, Nanjing, China). Total protein content was determined in the same sample by the bicinchoninic acid (BCA) method using the Pierce Protein Assay Kit (Thermo, Rockford, IL, USA).

Alizarin Red S (ARS) staining and quantification

Alizarin Red S staining and quantification were determined as described previously [21, 22]. After 14 days of osteogenic induction, cells were fixed with 4% paraformaldehyde for 20 min, washed three times with double-distilled water, and then stained with 2% ARS staining solution (pH 4.2; Sigma-Aldrich) for 30 min at room temperature. Images were obtained with a scanner. For the quantification of mineralization, the stain was solubilized with 100 mM cetylpyridinium chloride (Sigma-Aldrich) for 1 h and quantified by spectrophotometric absorbance at 562 nm.

RNA isolation and quantitative reverse transcription polymerase chain reaction (qRT-PCR)

The total RNA was extracted with TRIzol reagent (Invitrogen, Carlsbad, CA, USA) according to the manufacturer's instructions and then reverse-transcribed into cDNA using a cDNA Reverse Transcription Kit (Takara, Tokyo, Japan). Quantitative PCR was performed with SYBR Green Master Mix (Roche Applied Science, Mannheim, Germany) using a 7500 Real-Time PCR Detection System (Applied Biosystems, Foster City, CA, USA). The primers used for *MEG3*, miR-140-5p, osteocalcin (*OCN*), Runt-related transcription factor 2 (*RUNX2*), peroxisome proliferator-activated receptor- γ (*PPAR γ*), CCAAT-enhancer-binding proteins- α (*CEBP α*), *U6* (internal control for miRNAs), and glyceraldehyde 3-phosphate dehydrogenase (*GAPDH*, internal

control for mRNAs and lncRNAs) are listed in Table 1. The data were analyzed as described previously [23].

Western blot analysis

Western blot analysis was performed as described previously [23]. Briefly, cells were harvested, washed with PBS, and lysed in RIPA buffer. Proteins were separated by 10% sodium dodecyl sulfate polyacrylamide gel electrophoresis and transferred to nitrocellulose membranes. Primary antibodies against PPAR γ (Cell Signaling Technology, Beverly, MA, USA), OCN (Abcam, Cambridge, UK), and GAPDH (Abcam) were diluted in the ratio of 1:1,000. The membrane was incubated with goat anti-rabbit IgG (Abcam) and then visualized using ECL Western Blot Kit (CW BIO). Protein level was quantified using the National Institutes of Health ImageJ software (<https://imagej.nih.gov/ij/>). The background was subtracted and the signal of each target band was normalized to that of the GAPDH band.

Vector construction and luciferase reporter assay

The *MEG3* cDNA fragment containing the predicted potential miR-140-5p-binding sites were amplified by PCR method and cloned to PGL3-Enhancer luciferase vector (Promega, Madison, WI). The luciferase reporter vectors including PGL3-*MEG3* and PGL3-control vector were constructed by Integrated Biotech Solutions Company (Ibsbio). The *MEG3* sequence was cloned into the pcDNA3.1 vector by PCR method. The plasmid pcDNA-*MEG3* (or empty pcDNA) was transfected into cells for 48 h.

293T cells were grown in 48-well plates and cotransfected with 100 nM miR-140-5p mimic or control, 40 ng luciferase reporter plasmid (PGL3-*MEG3*, PGL3-control), and 4 ng pRL-TK, a plasmid expressing *Renilla* luciferase (Promega) using Lipofectamine 2000 (Invitrogen). The *Renilla* and firefly luciferase activities were measured 48 h after transfection using the Dual luciferase reporter assay system (Promega). All luciferase values were normalized to those of *Renilla* luciferase and expressed as fold-induction relative to the basal activity.

Heterotopic bone formation assay in vivo

hASCs were induced under osteogenic medium for 1 week before the in vivo study. Then, cells were collected, loaded onto Bio-Oss Collagen (Geistlich, GEWO GmbH, Baden-Baden, Germany) scaffolds and subsequently incubated at 37 °C for 3 h, followed by centrifugation at 150 g for 5 min and implanted subcutaneously on the dorsal space of 6-week-old, BALB/c homozygous nude (nu/nu) mice (ten mice per group), as described previously [21, 22]. This study was approved by the Institutional Animal

Care and Use Committee of the Peking University Health Science Center (LA2014233), and all animal experiments were performed in accordance with the Institutional Animal Guidelines.

Analyses of bone formation in vivo

After 8 weeks of implantation, implants were harvested and fixed in 4% paraformaldehyde. Specimens from each group were decalcified in 10% ethylene diamine tetraacetic acid (EDTA; pH 7.4) for 2 weeks, followed by dehydration and embedded in paraffin. Then, sections (5- μ m thickness) were cut and stained with hematoxylin and eosin (H&E) and Masson's trichrome. Tissue slices were visualized under a light microscope (Olympus Co., Tokyo, Japan).

Statistical analysis

Statistical analysis was performed using the SPSS Statistics 20.0 software (IBM, Armonk, NY). The results represented the mean of three independent experiments and data were presented as mean \pm standard deviation (SD). Comparisons between two groups were analyzed by Student's *t* test. For the testing of multiple groups, a one-way analysis of variance (ANOVA) was conducted. A two-tailed *P* value <0.05 was considered to indicate statistical significance.

Results

MEG3 expression is downregulated during adipogenic differentiation and upregulated during osteogenic differentiation of hASCs

The dynamic expression profiles of *MEG3* were detected in hASCs after induction to the adipocytic and osteoblastic lineages. The analysis of qRT-PCR showed that expression of *MEG3* was downregulated during the adipogenic differentiation of hASCs (Fig. 1a) and upregulated during osteogenic differentiation (Fig. 1b). The mRNA expression of adipogenesis-associated genes *PPAR γ* and *CEBP α* was significantly upregulated after adipogenesis (Fig. 1c, d). However, the osteogenic differentiation of hASCs was evidenced by the increased expression of osteogenesis-associated genes, namely, *RUNX2* and *OCN* at the indicated time (Fig. 1e, f).

Knockdown of *MEG3* promotes adipocyte differentiation

To investigate the functions of *MEG3* in the adipogenic differentiation of hASCs, we established *MEG3* knockdown hASCs using lentivirus transfection. The

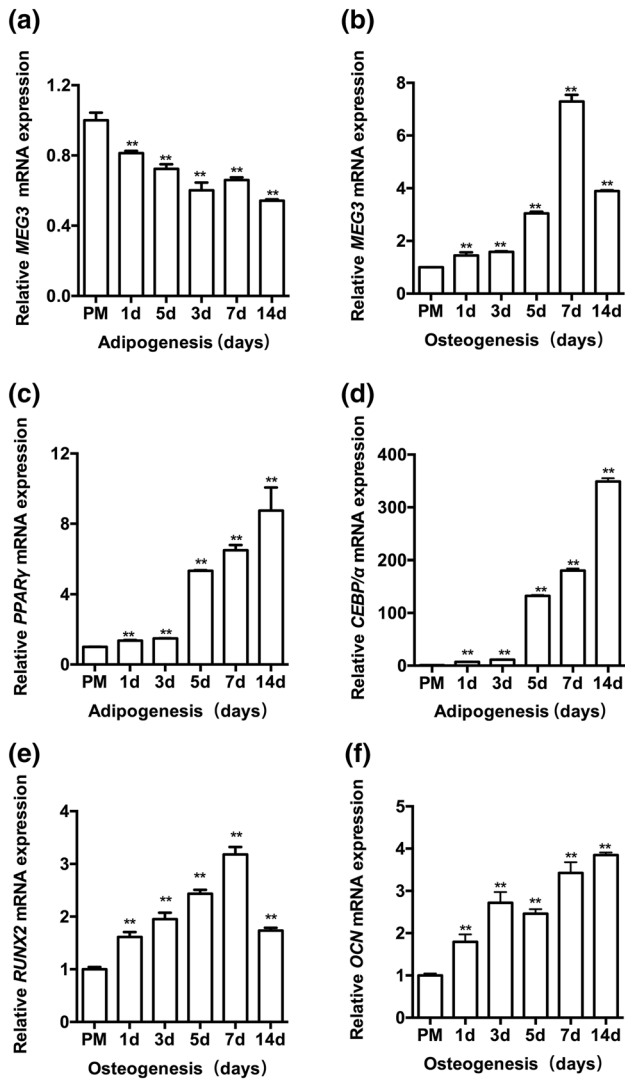


Fig. 1 Expression profiles of lncRNA *MEG3* during adipogenic and osteogenic differentiation of hASCs at the indicated time points. **a** Relative expression of *MEG3* during adipogenic differentiation as determined by qRT-PCR analysis. **b** Relative expression of *MEG3* during osteogenic differentiation. **c, d** Relative mRNA expression levels of the adipogenic markers *PPAR γ* , *CEBP α* at the indicated time points. **e, f** Relative mRNA expression levels of *RUNX2*, *OCN* expression was increased during the osteogenic differentiation of human adipose-derived stem cells (hASCs). Results are presented as mean \pm SD (* P < 0.05, ** P < 0.01)

stably expressing cells were sorted into NC and sh-*MEG3* groups. Lentiviral transduction efficiency was estimated to be more than 80% as evaluated by the percentage of GFP-positive cells after transduction (Fig. 2a). The qRT-PCR confirmed a significant decrease in the sh-*MEG3* group compared with the NC group (Fig. 2b). Oil Red O staining and quantification showed that knockdown of *MEG3* promoted the adipocyte formation of hASCs on day 10 of adipogenic differentiation (Fig. 2c). Moreover, knockdown of *MEG3* significantly upregulated

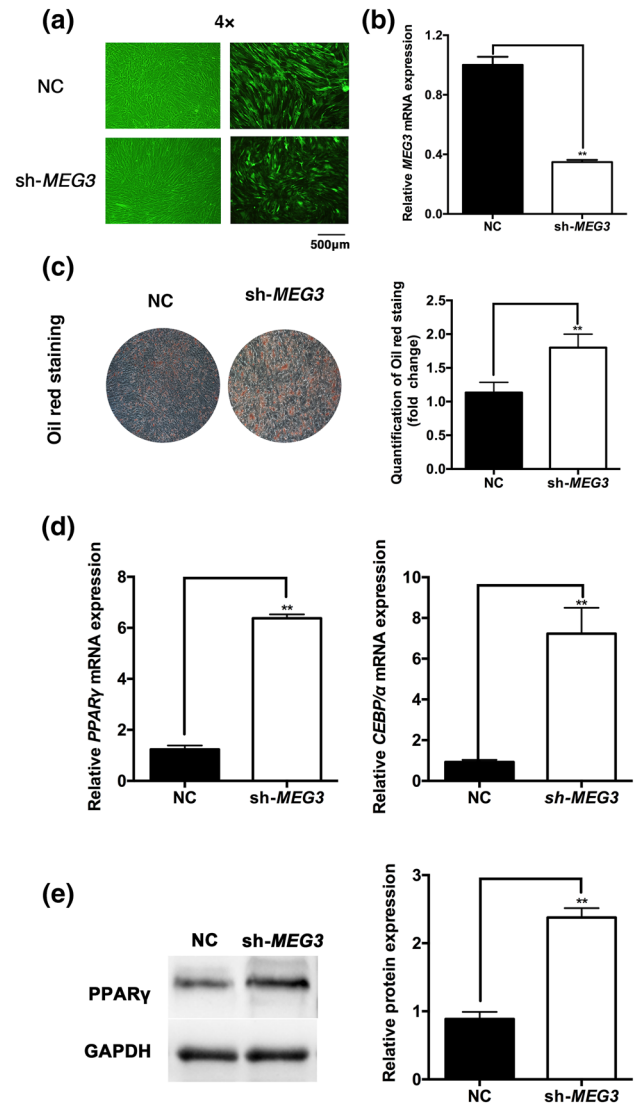


Fig. 2 Knockdown of *MEG3* promotes the adipogenic differentiation of hASCs. **a** Micrographs of GFP-positive hASCs under ordinary and fluorescent light in the NC and sh-*MEG3* groups. Scale bar 500 μ m. **b** Knockdown efficiency of *MEG3* in hASCs expressing sh-*MEG3* as determined by qRT-PCR. **c** Images of Oil Red O staining in hASCs transfected with sh-*MEG3* and its control vector (NC) after 10 days of adipogenic differentiation. Histograms show quantitation of Oil Red O staining by spectrophotometry (normalized to control groups). **d** Relative mRNA expression of the adipogenic factors *PPAR γ* , *CEBP α* measured by qRT-PCR on day 10 of adipogenic induction in hASCs transfected with sh-*MEG3* and NC. *GAPDH* was used for normalization. **e** Western blot analysis of *PPAR γ* and *GAPDH* on day 10 of adipogenic induction in hASCs transfected with sh-*MEG3* and NC. *GAPDH* was used as the internal control. Histograms show quantification of the band intensities. Results are presented as mean \pm SD (* P < 0.05, ** P < 0.01)

the mRNA expression of the adipogenesis-associated genes, *PPAR γ* and *CEBP α* after 10 days of adipogenic differentiation (Fig. 2d). Western blot analysis indicated the similar tendency with *PPAR γ* expression in the

sh-*MEG3* group after 10 days of adipogenic differentiation (Fig. 2e).

Knockdown of *MEG3* inhibits the osteogenic differentiation of hASCs

To evaluate the functions of *MEG3* in the osteogenic differentiation of hASCs, we further induced *MEG3*-knockdown hASCs into the osteoblastic lineage. ALP staining and activity assay showed that knockdown of *MEG3* decreased the osteogenic differentiation of hASCs on day 7 (Fig. 3a, b). ARS staining and quantification indicated that the calcium deposition of induced hASCs was reduced in the sh-*MEG3* group on day 14 (Fig. 3a, b). The qRT-PCR

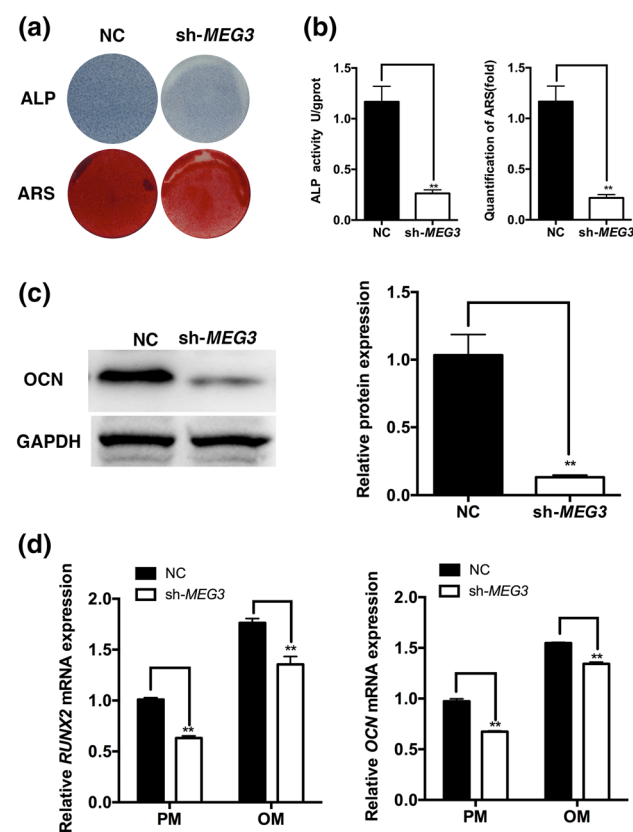


Fig. 3 Knockdown of *MEG3* inhibits the osteogenic differentiation of hASCs. **a** Images of ALP staining on day 7 and Alizarin Red S (ARS) staining on day 14 after osteogenic induction in hASCs transfected with sh-*MEG3* and NC. **b** ALP activity on day 7 and ARS mineralization assay on day 14 after osteogenic induction in hASCs transfected with sh-*MEG3* and NC. Histograms show the quantification of ARS staining by spectrophotometry. **c** Western blot analysis of OCN after 14 days of osteogenic induction in hASCs transfected with sh-*MEG3* and NC. GAPDH was used as the internal control. Histograms show the quantification of band intensities. **d** Relative mRNA expression of *RUNX2* and *OCN* was measured by qRT-PCR on day 14 of osteogenic induction in hASCs transfected with sh-*MEG3* and NC. GAPDH was used for normalization. Results are presented as mean \pm SD (* P < 0.05, ** P < 0.01)

analysis showed that the mRNA expression of osteogenesis-associated genes, *RUNX2* and *OCN* was significantly decreased in the sh-*MEG3* group (Fig. 3d). Similarly, the protein expression of OCN was also decreased in *MEG3*-knockdown hASCs cultured in osteogenic medium (OM) for 14 days (Fig. 3c).

Moreover, hASCs transfected with sh-*MEG3* or NC were loaded onto Bio-Oss Collagen scaffolds, and transplanted into the subcutaneous space of nude mice (6-week-old). After 8 weeks, the transplants were harvested and then subjected to histological analysis. H&E staining showed that new bone formation was much less in the sh-*MEG3* group than that in the NC group (Fig. s1b). Masson's trichrome staining revealed that the collagen organization with blue color was also lower in the sh-*MEG3* group (Fig. s1b).

The relationship between *MEG3* and miR-140-5p

According to the previous study, the *MEG3* transcript contains a conserved putative target binding site of miR-140-5p in its 3'-UTR. Therefore, we constructed luciferase reporter plasmids containing the miR-140-5p target site in the *MEG3* 3'-UTR sequence. Overexpression of miR-140-5p significantly suppressed the firefly luciferase activity of the reporter of PGL3-*MEG3* group, but

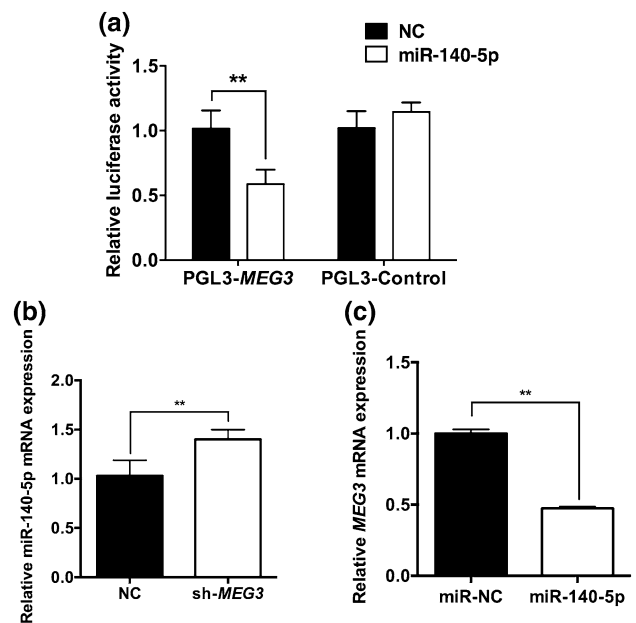


Fig. 4 The relationship between *MEG3* and miR-140-5p. **a** Relative luciferase activity of cells with miR-140-5p mimics in PGL3-*MEG3* and PGL3-control groups. **b** Relative expression of miR-140-5p measured by qRT-PCR in hASCs transfected with sh-*MEG3* and the control vector. *U6* was used for normalization. **c** Relative expression of *MEG3* measured by qRT-PCR in hASCs transfected with miR-140-5p and the control vector. GAPDH was used for normalization. Results are presented as mean \pm SD (* P < 0.05, ** P < 0.01)

Fig. 5 miR-140-5p promotes the adipogenic differentiation of hASCs. **a** Images of Oil Red O staining in hASCs transfected with miR-140-5p, anti-miR-140-5p, or their scrambled vectors (miR-NC, anti-NC) on day 10 of adipogenic differentiation. **b** Histograms show quantification of Oil Red O staining by spectrophotometry. **c** Overexpression/knockdown efficiency of miR-140-5p in hASCs. **d** Relative mRNA expression of the adipogenic factors *PPAR γ* , *CEBP α* measured by qRT-PCR on day 10 of adipogenic induction in hASCs transfected with miR-140-5p, anti-miR-140-5p, or their scrambled vectors (miR-NC, anti-NC). *GAPDH* was used for normalization. **e** Western blot analysis of *PPAR γ* and *GAPDH* on day 10 of adipogenic induction in hASCs transfected with miR-140-5p, anti-miR-140-5p, or their scrambled vectors (miR-NC, anti-NC). *GAPDH* was used as the internal control. Histograms show quantification of the band intensities. Results are presented as mean \pm SD (* P < 0.05, ** P < 0.01)

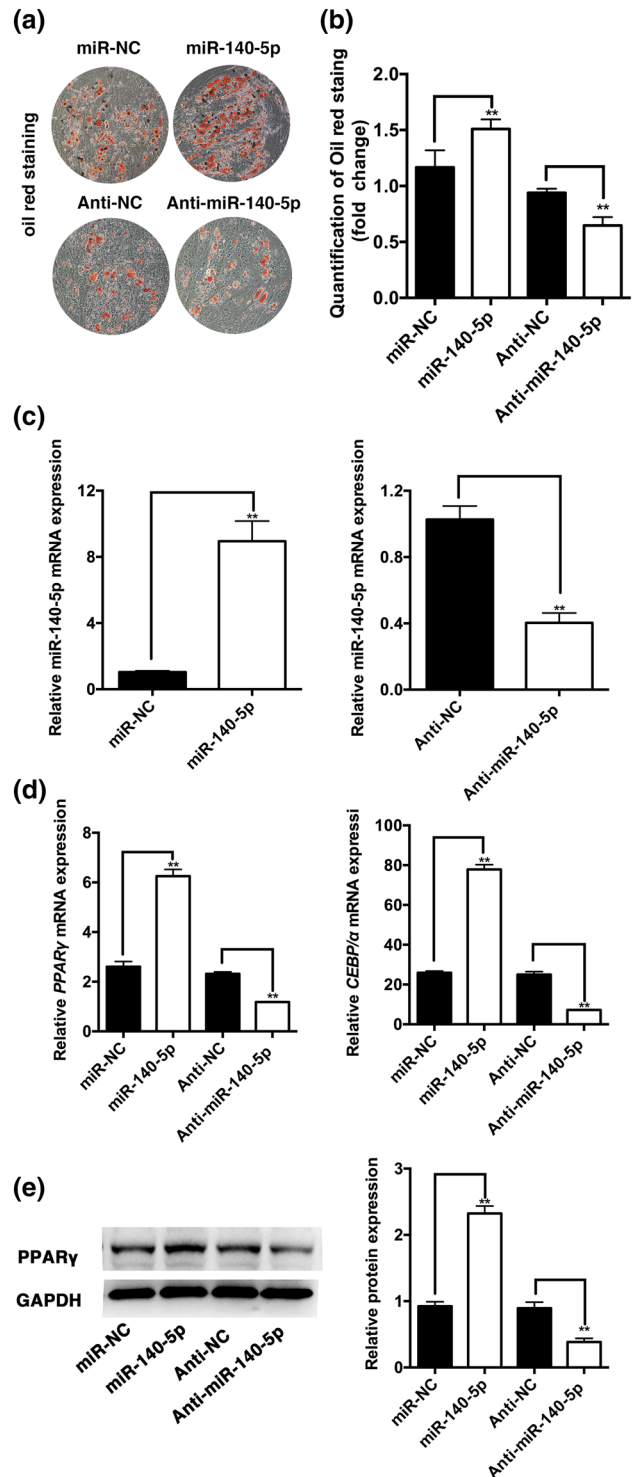
not that of PGL3-control group (Fig. 4a). Subsequently, we detected the expression level of miR-140-5p after knockdown of *MEG3*, and the results showed that the expression of miR-140-5p was significantly increased in hASCs transfected with sh-*MEG3* compared with control cells (Fig. 4b). In contrast, overexpression of miR-140-5p led to downregulation of *MEG3* expression in hASCs (Fig. 4c).

miR-140-5p is involved in the adipogenic and osteogenic lineage differentiation of hASCs

To further investigate the involvement of miR-140-5p in the multilineage differentiation of hASCs, lentiviruses were transfected to overexpress or knockdown miR-140-5p in hASCs. The efficiency of lentiviral transduction was estimated to be more than 80% (Fig. s1a). The qRT-PCR analysis of miR-140-5p expression confirmed an almost tenfold increase in the miR-140-5p overexpression group (miR-140-5p), and a 60% decrease in the miR-140-5p knockdown group (Anti-miR-140-5p) (Fig. 5c).

After induction to the adipogenic lineage, Oil Red O staining and quantification indicated that overexpression of miR-140-5p promoted the adipocyte formation of hASCs, whereas knockdown of miR-140-5p showed the opposite effect on day 10 (Fig. 5a, b). Moreover, qRT-PCR analysis revealed that the mRNA expression of *PPAR γ* and *CEBP α* was significantly upregulated in the miR-140-5p group and downregulated in the anti-miR-140-5p group on day 10 (Fig. 5d). Western blot analysis indicated the similar tendency with the protein expression of *PPAR γ* on 10 days of adipogenic differentiation (Fig. 5e).

Moreover, after induction to the osteogenic lineage, ALP staining and activity assay showed that overexpression of miR-140-5p inhibited the osteogenic differentiation of hASCs, while knockdown of miR-140-5p enhanced hASCs osteogenesis on day 7 (Fig. 6a, b). ARS staining and quantification demonstrated the similar tendency on day 14 (Fig. 6a, b). The qRT-PCR analysis indicated the mRNA



levels of *RUNX2* and *OCN* were decreased with miR-140-5p overexpression, whereas the opposite effects were observed in the anti-miR-140-5p group (Fig. 6c).

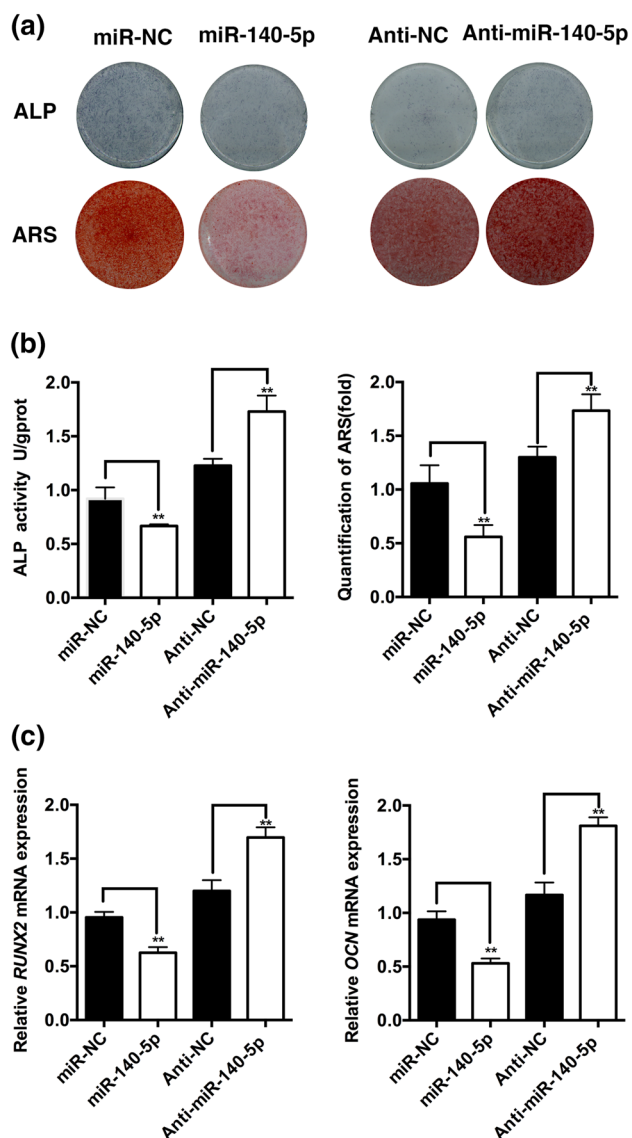


Fig. 6 miR-140-5p inhibits the osteogenic differentiation of hASCs. **a** Images of ALP staining on day 7 and Alizarin Red S (ARS) staining on day 14 of osteogenic induction hASCs transfected with miR-140-5p, anti-miR-140-5p, or the scrambled vectors (miR-NC, anti-NC). **b** Histograms show the activity of ALP and quantification of ARS staining by spectrophotometry in hASCs transfected with miR-140-5p, anti-miR-140-5p, or the scrambled vectors (miR-NC, anti-NC). **c** Relative mRNA expression of *RUNX2* and *OCN* was measured by qRT-PCR on day 14 of osteogenic induction in hASCs transfected with miR-140-5p, anti-miR-140-5p, or the scrambled vectors (miR-NC, anti-NC). *GAPDH* was used for normalization. Results are presented as mean \pm SD (* P < 0.05, ** P < 0.01)

Discussion

Here, we demonstrated that knockdown of lncRNA *MEG3* enhanced adipogenesis in hASCs. *MEG3* has been identified as an important regulator of osteogenesis that upregulation of *MEG3* promoted osteogenic differentiation by

targeting *BMP4* transcription in BMSCs [18]. However, limited knowledge is available pertaining to the roles of *MEG3* regulating adipocyte differentiation in hASCs. Several researches suggest a reciprocal relationship between the adipocytic and osteoblastic lineages and that a mutually inhibitory relationship exists between fat accumulation and bone deficiency [24]. And the balance of them is tightly regulated by multiple signaling pathways [25–28]. Our study showed that *MEG3* played essential roles in the regulatory networks of adipogenesis in hASCs. Thus, *MEG3* might act as a switch of adipogenesis and osteogenesis to maintain the balance of MSC differentiation, which provides a potential target for treating metabolic disorders, such as bone loss and lipid accumulation.

Although a previous study has reported that *MEG3* promoted osteogenic differentiation of BMSCs [18], its functions in hASCs osteogenesis remain unclear. Our study examined the dynamic profiles of *MEG3* expression during osteogenesis, showing that it was significantly upregulated during osteogenesis of hASCs. As a type of adult mesenchymal stem cells, hASCs share many biological characteristics with BMSCs [29, 30] and possess attractive characters for clinical application compared to BMSCs such as abundant stem cells resources, faster growth and less pain and morbidity during surgery [31]. However, several studies based on profiling strategy have highlighted discrepancies at transcription and proteomic levels between BMSCs and ASCs concerning regulation of adipogenic and osteogenic differentiation [32–35]. A myriad of differentially expressed genes are presented in Wnt signaling, PPAR signaling, and other important pathways between these two types of MSCs, indicating a divergence in signaling regulation programs between them [36, 37]. Some functional studies have confirmed that BMSCs and ASCs adopt different patterns of gene regulation programs for osteogenic differentiation. For example, miR-26a targeted on *GSK3 β* to activate Wnt signaling to promote osteogenic differentiation of BMSCs, while exerted inhibitory role of hASCs osteogenesis by suppressing BMP signaling, suggesting distinct post-transcriptional regulation of tissue-specific MSCs differentiation [38]. Therefore, there may be multiple signaling pathways and diverse intrinsic molecules involved during the regulation of hASCs adipogenic and osteogenic differentiation by *MEG3*.

The regulatory mechanisms governing lncRNAs are diversified and complicated, including co-transcriptional regulation, gene expression, and scaffolding of nuclear or cytoplasmic complexes [39–41]. For instance, lncRNA *H19* and *H19*-derived miR-675 inhibit the adipogenic differentiation of BMSCs through the epigenetic modulation of hASCs [3]. lncRNA *MIR31HG* regulated bone formation and inflammation via regulatory circuitry of NF- κ B [42]. Recently, it has been found that lncRNAs could regulate

miRNA expression via direct competition for miRNA binding [38, 43], subsequently modulating the target genes of miRNAs in post-transcriptional level, and thus acting as competing endogenous RNAs (ceRNAs) [22]. *MEG3* may function as a ceRNA to bind with miRNAs, such as miR-21-5p [44], miR-181 [45], miR-106b [46], and miR-140-5p [47]. Among them, miR-140-5p has been demonstrated as an essential regulator during adipogenesis [48] and osteogenesis [19] in different cell lines. Consistent with the previous reports, our results demonstrated that overexpression of miR-140-5p promoted adipogenic differentiation and inhibited osteogenic differentiation of hASCs, while knock-down of miR-140-5p represented opposite roles. Moreover, the expression of miR-140-5p was inversely correlated with *MEG3* expression. This study showed that *MEG3* might regulate miR-140-5p during adipogenic and osteogenic differentiation of hASCs.

In conclusion, *MEG3* plays important roles in the adipogenic and osteogenic balance during the multilineage differentiation of hASCs. The mechanism may be at least partially through regulating miR-140-5p. However, as lncRNAs act via a variety of mechanisms, *MEG3* may also interact with other molecules involved in the complex biologic regulation network of adipogenic and osteogenic differentiation of hASCs. Profound investigations may elucidate whether *MEG3* and miR-140-5p modulate the shift of cell lineage commitment of hASCs and provide potential therapeutic targets for metabolic-related disorders.

Author contributions ZL and CJ: performed the experiments and wrote the paper; SC, YZ, and YH: revised the paper, collection and assembly of the data; LJ and WG: conception and design, financial support, and final approval of the manuscript. YZ: financial support, revised the paper, and final approval of the manuscript.

Funding This study was financially supported by grants from the National Natural Science Foundation of China (81371118, 81200763, 81670963), the Ph.D. Programs Foundation of Ministry of Education of China (20130001110101), the Project for Culturing Leading Talents in Scientific and Technological Innovation of Beijing (Z171100001117169), and the grant of Peking University School and Hospital of Stomatology (PKUSS20140104).

Compliance with ethical standards

Conflict of interest The authors have no conflict of interest to disclose.

References

- Rumman M, Dhawan J, Kassem M (2015) Concise review: quiescence in adult stem cells: biological significance and relevance to tissue regeneration. *Stem Cells* 33(10):2903–2912. doi:10.1002/stem.2056
- Muruganandan S, Roman AA, Sinal CJ (2009) Adipocyte differentiation of bone marrow-derived mesenchymal stem cells: cross talk with the osteoblastogenic program. *Cell Mol Life Sci* 66(2):236–253. doi:10.1007/s00018-008-8429-z
- Huang Y, Zheng Y, Jin C, Li X, Jia L, Li W (2016) Long non-coding RNA H19 inhibits adipocyte differentiation of bone marrow mesenchymal stem cells through epigenetic modulation of histone deacetylases. *Sci Rep* 6:28897. doi:10.1038/srep28897
- Wilusz JE, Sunwoo H, Spector DL (2009) Long noncoding RNAs: functional surprises from the RNA world. *Genes Dev* 23(13):1494–1504. doi:10.1101/gad.1800909
- Bartel D (2009) MicroRNAs: target recognition and regulatory functions. *Cell* 136(2):215–233
- Li J, Meng H, Bai Y, Wang K (2016) Regulation of lncRNA and its role in cancer metastasis. *Oncol Res* 23(5):205–217. doi:10.3727/096504016x14549667334007
- Wang L, Wu F, Song Y, Li X, Wu Q, Duan Y, Jin Z (2016) Long noncoding RNA related to periodontitis interacts with miR-182 to upregulate osteogenic differentiation in periodontal mesenchymal stem cells of periodontitis patients. *Cell Death Dis* 7(8):e2327
- Huang J, Zhao L, Xing L, Chen D (2010) MicroRNA-204 regulates Runx2 protein expression and mesenchymal progenitor cell differentiation. *Stem Cells* 28(2):357–364. doi:10.1002/stem.288
- Zhang JF, Fu WM, He ML, Wang H, Wang WM, Yu SC, Bian XW, Zhou J, Lin MC, Lu G (2011) miR-637 maintains the balance between adipocytes and osteoblasts by directly targeting Osterix. *Mol Biol Cell* 22(21):3955–3961
- Jeong BC, Kang IH, Hwang YC, Kim SH, Koh JT (2014) MicroRNA-194 reciprocally stimulates osteogenesis and inhibits adipogenesis via regulating COUP-TFII expression. *Cell Death Dis* 5:e1532. doi:10.1038/cddis.2014.485
- Divoux A, Karastergiou K, Xie H, Guo W, Perera RJ, Fried SK, Smith SR (2014) Identification of a novel lncRNA in gluteal adipose tissue and evidence for its positive effect on preadipocyte differentiation. *Obesity (Silver Spring)* 22(8):1781–1785. doi:10.1002/oby.20793
- Li M, Sun X, Cai H, Sun Y, Plath M, Li C, Lan X, Lei C, Lin F, Bai Y, Chen H (2016) Long non-coding RNA ADNCR suppresses adipogenic differentiation by targeting miR-204. *Biochim Biophys Acta* 1859(7):871–882. doi:10.1016/j.bbagr.2016.05.003
- Benetatos L, Vartholomatos G, Hatzimichael E (2011) *MEG3* imprinted gene contribution in tumorigenesis. *Int J Cancer* 129(4):773–779
- Wang P, Ren Z, Sun P (2012) Overexpression of the long non-coding RNA *MEG3* impairs in vitro glioma cell proliferation. *J Cell Biochem* 113(6):1868–1874
- Anwar SL, Krech T, Hasemeier B, Schipper E, Schweitzer N, Vogel A, Kreipe H, Lehmann U (2012) Loss of imprinting and allelic switching at the *DLK1-MEG3* locus in human hepatocellular carcinoma. *PLoS One* 7(11):e49462. doi:10.1371/journal.pone.0049462
- Boon RA, Hofmann P, Michalik KM, Lozano-Vidal N, Berghauer D, Fischer A, Knau A, Jae N, Schurmann C, Dimmeler S (2016) Long noncoding RNA *Meg3* controls endothelial cell aging and function: implications for regenerative angiogenesis. *J Am Coll Cardiol* 68(23):2589–2591. doi:10.1016/j.jacc.2016.09.949
- Kameswaran V, Bramswig NC, McKenna LB, Penn M, Schug J, Hand NJ, Chen Y, Choi I, Vourekas A, Won KJ (2014) Epigenetic regulation of the *DLK1-MEG3* microRNA cluster in human type 2 diabetic islets. *Cell Metab* 19(1):135–145
- Zhuang W, Ge X, Yang S, Huang M, Zhuang W, Chen P, Zhang X, Fu J, Qu J, Li B (2015) Upregulation of lncRNA *MEG3* promotes osteogenic differentiation of mesenchymal stem cells from multiple myeloma patients by targeting *BMP4* transcription. *Stem Cells* 33(6):1985–1997

19. Hwang S, Park SK, Lee HY, Kim SW, Lee JS, Choi EK, You D, Kim CS, Suh N (2014) miR-140-5p suppresses BMP2-mediated osteogenesis in undifferentiated human mesenchymal stem cells. *FEBS Lett* 588(17):2957–2963
20. Zhang P, Liu Y, Jin C, Zhang M, Tang F, Zhou Y (2016) Histone acetyltransferase GCN5 regulates osteogenic differentiation of mesenchymal stem cells by inhibiting NF-kappaB. *J Bone Miner Res* 31(2):391–402. doi:10.1002/jbmr.2704
21. Ge W, Liu Y, Chen T, Zhang X, Lv L, Jin C, Jiang Y, Shi L, Zhou Y (2014) The epigenetic promotion of osteogenic differentiation of human adipose-derived stem cells by the genetic and chemical blockade of histone demethylase LSD1. *Biomaterials* 35(23):6015–6025. doi:10.1016/j.biomaterials.2014.04.055
22. Ge W, Shi L, Zhou Y, Liu Y, Ma GE, Jiang Y, Xu Y, Zhang X, Feng H (2011) Inhibition of osteogenic differentiation of human adipose-derived stromal cells by retinoblastoma binding protein 2 repression of RUNX2-activated transcription. *Stem Cells* 29(7):1112–1125. doi:10.1002/stem.663
23. Jia LF, Wei SB, Gan YH, Guo Y, Gong K, Mitchelson K, Cheng J, Yu GY (2014) Expression, regulation and roles of miR-26a and MEG3 in tongue squamous cell carcinoma. *Int J Cancer* 135(10):2282–2293. doi:10.1002/ijc.28667
24. Greco EA, Lenzi A, Migliaccio S (2015) The obesity of bone. *Ther Adv Endocrinol Metab* 6(6):273
25. Pino AM, Rosen CJ, Rodríguez JP (2012) In osteoporosis, differentiation of mesenchymal stem cells (MSCs) improves bone marrow adipogenesis. *Biol Res* 45(3):279–287
26. Jeong BC, Kang IH, Hwang YC, Kim SH, Koh JT (2014) MicroRNA-194 reciprocally stimulates osteogenesis and inhibits adipogenesis via regulating COUP-TFII expression. *Cell Death Dis* 5(5):e1532
27. Liu HZ, Wang QY, Zhang Y, Qi DT, Li MW, Guo WQ, Ma YH, Wang LY, Chen Y, Gao CY (2016) Pioglitazone up-regulates long non-coding RNA MEG3 to protect endothelial progenitor cells via increasing HDAC7 expression in metabolic syndrome. *Biomed Pharmacother* 78:101–109. doi:10.1016/j.biopha.2016.01.001
28. Moerman EJ, Teng K, Lipschitz DA, Lecka-Czernik B (2004) Aging activates adipogenic and suppresses osteogenic programs in mesenchymal marrow stroma/stem cells: the role of PPAR-gamma2 transcription factor and TGF-beta/BMP signaling pathways. *Aging Cell* 3(6):379–389. doi:10.1111/j.1474-9728.2004.00127.x
29. Gómezbarrena E, Rosset P, Müller I, Giordano R, Bunu C, Layrolle P, Konttinen YT, Luyten FP (2011) Bone regeneration: stem cell therapies and clinical studies in orthopaedics and traumatology. *J Cell Mol Med* 15(6):1266–1286
30. Wei CC, Lin AB, Hung SC (2014) Mesenchymal stem cells in regenerative medicine for musculoskeletal diseases: bench, bedside, and industry. *Cell Transplant* 23(4–5):505–512. doi:10.3727/096368914x678328
31. Liao HT, Chen CT (2014) Osteogenic potential: comparison between bone marrow and adipose-derived mesenchymal stem cells. *World J Stem Cells* 6(3):288–295. doi:10.4252/wjsc.v6.i3.288
32. Monaco E, Bionaz M, Rodriguez-Zas S, Hurley WL, Wheeler MB (2012) Transcriptomics comparison between porcine adipose and bone marrow mesenchymal stem cells during in vitro osteogenic and adipogenic differentiation. *PLoS One* 7(3):e32481
33. Park SH, Sim WY, Min BH, Yang SS, Khademhosseini A, Kaplan DL (2012) Chip-based comparison of the osteogenesis of human bone marrow- and adipose tissue-derived mesenchymal stem cells under mechanical stimulation. *PLoS One* 7(9):e46689
34. Strioga M, Viswanathan S, Darinkas A, Slaby O, Michalek J (2012) Same or not the same? Comparison of adipose tissue-derived versus bone marrow-derived mesenchymal stem and stromal cells. *Stem Cells Dev* 21(14):2724–2752
35. Noël D, Caton D, Roche S, Bony C, Lehmann S, Casteilla L, Jorgensen C, Cousin B (2008) Cell specific differences between human adipose-derived and mesenchymal-stromal cells despite similar differentiation potentials. *Exp Cell Res* 314(7):1575
36. Dreyer C, Krey G, Keller H, Givel F, Helftenbein G, Wahli W (1992) Control of the peroxisomal beta-oxidation pathway by a novel family of nuclear hormone receptors. *Cell* 68(5):879–887
37. Takada I, Kouzmenko AP, Kato S (2009) Wnt and PPARgamma signaling in osteoblastogenesis and adipogenesis. *Nat Rev Rheumatol* 5(8):442
38. Su X, Liao L, Shuai Y, Jing H, Liu S, Zhou H, Liu Y, Jin Y (2015) miR-26a functions oppositely in osteogenic differentiation of BMSCs and ADSCs depending on distinct activation and roles of Wnt and BMP signaling pathway. *Cell Death Dis* 6(8):e1851
39. Ulitsky I, Bartel DP (2013) lincRNAs: genomics, evolution, and mechanisms. *Cell* 154(1):26–46
40. Wilusz JE (2016) Long noncoding RNAs: re-writing dogmas of RNA processing and stability. *Biochim Biophys Acta* 1859(1):128–138. doi:10.1016/j.bbagr.2015.06.003
41. Housman G, Ulitsky I (2016) Methods for distinguishing between protein-coding and long noncoding RNAs and the elusive biological purpose of translation of long noncoding RNAs. *Biochim Biophys Acta* 1859(1):31–40. doi:10.1016/j.bbagr.2015.07.017
42. Jin C, Jia L, Huang Y, Zheng Y, Du N, Liu Y, Zhou Y (2016) Inhibition of lincRNA MIR31HG promotes osteogenic differentiation of human adipose-derived stem cells. *Stem Cells* 34(11):2707–2720
43. Nie FQ, Zhu Q, Xu TP, Zou YF, Xie M, Sun M, Xia R, Lu KH (2014) Long non-coding RNA MVIH indicates a poor prognosis for non-small cell lung cancer and promotes cell proliferation and invasion. *Tumor Biol* 35(8):7587–7594
44. Zhang J, Yao T, Wang Y, Yu J, Liu Y, Lin Z (2016) Long non-coding RNA MEG3 is downregulated in cervical cancer and affects cell proliferation and apoptosis by regulating miR-21. *Cancer Biol Ther* 17(1):104–113. doi:10.1080/15384047.2015.1108496
45. Peng W, Si S, Zhang Q, Li C, Zhao F, Wang F, Yu J, Ma R (2015) Long non-coding RNA MEG3 functions as a competing endogenous RNA to regulate gastric cancer progression. *J Exp Clin Cancer Res* 34(1):1–10
46. Zheng L, Zhang Y, Lin S, Sun A, Chen R, Ding Y, Ding Y (2015) Down-regulation of miR-106b induces epithelial-mesenchymal transition but suppresses metastatic colonization by targeting Prrx1 in colorectal cancer. *Int J Clin Exp Pathol* 8(9):10534–10544
47. Liu HZ, Wang QY, Zhang Y, Qi DT, Li MW, Guo WQ, Ma YH, Wang LY, Chen Y, Gao CY (2016) Pioglitazone up-regulates long non-coding RNA MEG3 to protect endothelial progenitor cells via increasing HDAC7 expression in metabolic syndrome. *Biomed Pharmacother* 78:101–109
48. Zhang X, Chang A, Li Y, Gao Y, Wang H, Ma Z, Li X, Wang B (2015) miR-140-5p regulates adipocyte differentiation by targeting transforming growth factor-β signaling. *Sci Rep* 5(2):18118